Molecular Crystals and Liquid Crystals
Publication details, including instructions for authors and subscription information:
http://www.tandfonline.com/loi/gmcl16

Structural Imperfections as Triplet Exciton Traps in Anthracene Crystals

Kohei Yokoi [a] & Yujiro Ohba [a]
[a] Department of Instrumentation Engineering, Faculty of Science and Technology, Keio University, Kohoku-Ku, Yokohama, 223, Japan
Version of record first published: 20 Apr 2011.

To cite this article: Kohei Yokoi & Yujiro Ohba (1986): Structural Imperfections as Triplet Exciton Traps in Anthracene Crystals, Molecular Crystals and Liquid Crystals, 141:1-2, 151-163

To link to this article: http://dx.doi.org/10.1080/00268948608080206

Mol. Cryst. Liq. Cryst., 1986, Vol. 141, pp. 151–163
0026-8941/86/1412-0151/$20.00/0

Printed in the United States of America

Structural Imperfections as Triplet Exciton Traps in Anthracene Crystals

KOHEI YOKOI and YUJIRO OHBA

Department of Instrumentation Engineering, Faculty of Science and Technology, Keio University, Kohoku-ku, Yokohama 223, Japan

(*Received January 21, 1986; in final form April 15, 1986*)

Structural imperfections were generated in anthracene single crystals at 93 K by plastic bending and thermal stress. The number of stages in the triplet exciton traps and the anneal characteristics of the defects were measured at 93–423 K and then analyzed quantitatively. The depth of the triplet exciton trap (0.37, 0.26 eV) and the activation energies for defect-recovery (1.34, 1.09 eV) were obtained for ((001) [010] and (001) [100]) edge dislocations, introduced by bending along the *a* and *b* crystal axis, respectively. Each dislocation is accompanied by one or two shallower traps. Thermal defects consisted of all traps observed in the mechanically-deformed samples plus two other traps annealed at below room temperature.

Keywords: anthracene, crystal defects, triplet excitons, trapping, annealing, activation energy

1. INTRODUCTION

It has been clarified that a considerable number of structural imperfections, such as dislocations, still remain in anthracene single crystals, even if exceptional care is taken in the purification and subsequent crystal growth. These defects act as local trapping centers for charge carriers and excitons, enabling them to be observed using electrical or optical excitation methods in addition to direct observation, such as optical microscopy, X-ray topography, or transmission electron microscopy.

Degrees of potential disorders for the triplet exciton in structural imperfections are smaller than those for the singlet exciton and charge carriers. However, the lifetime of the triplet exciton is much longer than that of the singlet exciton; Triplet excitation is free from the

problems of crystal surface disorder against singlet excitation or injection of charge carriers. These characteristics of the triplet exciton make it possible to detect low level defects in bulk crystal. The behavior of the triplet exciton appears as delayed fluorescence resulting from triplet–triplet annihilation in addition to phosphorescence.

The method of investigating defects using delayed fluorescence was virtually developed by Siebrand[1] and has spread widely. He analyzed kinetically the temperature dependence of the intensity of the delayed fluorescence measured by Singh and Lipsett[2] using the concept of multi-level triplet exciton trapping. Arnold et al.[3] extended the method to the delayed fluorescence lifetime, which is one half of the triplet lifetime. Though several investigations by similar methods have been carried out,[4–7] Arnold et al.,[3] Goode et al.,[8] and Sasaki and Hayakawa[9] applied this method to the edge dislocation (001)[010], a well-known defect.

This method has advantages when used for nonradiative traps, which are not detectable by defect fluorescence or defect phosphorescence. However, for radiative traps, the accuracy of measurement of trap depth and the lifetime of the trapped excitation is inferior to that using spectroscopic methods, since it is an indirect method.

On the other hand, by thermal treatment, excess structural imperfections are removed, as certified directly by Kojima et al.[10] by observing etch-pit density. An alternative way of studying structural imperfections is to measure and analyze the anneal characteristics of the exciton traps.

In this paper, we analyze the structural imperfections introduced by mechanical and thermal deformation by looking at triplet exciton trapping and study the recovery of the defects. The results for dislocations were compared with those for thermal defects.

2. EXPERIMENTAL

Samples were anthracene single crystals melt-grown by the Bridgman method after refinement by column chromatography and zone-refining of about 100 passes. They were typically 1 mm thick and 5 mm square *ab* plane cleaved platelets with room-temperature triplet lifetime ~20 ms. Edge dislocations were generated by plastic bending using guides, similar to the method used by Sasaki and Hayakawa.[9] We did not observe any etch-pits. However the generation of edge dislocations can be taken for granted as shown by Robinson.[11] The types of dislocations generated are: a (001)[010] basal edge dis-

location when the direction of the knife edge used is parallel to the *a* axis on the *ab* plane, and a (001)[100] basal edge dislocation when the knife edge is parallel to the *b* axis.

The delayed fluorescence was measured by a real-time photon counting system synchronized with chopped excitation light from a He-Ne laser. The decay data was integrated 400 times for the measurement of exciton trap stages, and 4000 times for the measurement of anneal characteristics. The triplet decay rate, i.e. the reciprocal of the triplet lifetime, was taken as half of the decay rate of the delayed fluorescence.

Experiments consisted of the following two parts.

2.1. Measurement of exciton trap stages

In order to perform both plastic bending at 93 K and the measurement of delayed fluorescence without removing the sample from the cryostat, the mechanism shown in Figure 1 was used. As the sample was sandwiched by two thin steel plates, it could be returned to the original position after bending and removing the knife edge. The knife edge and the excitation light were parallel to each other; and the delayed fluorescence was measured in a direction perpendicular to them. The deformation may not be uniform within the sample in the direction perpendicular to the excitation light. However, because the excitation light spot was about 1 mm in diameter, much smaller than the size of the sample, this does not pose a problem.

Thermal defects were introduced by dipping the sample into a liquid nitrogen dewar after holding it in air in the dark at 423 K for several minutes. The sample in the dewar was transferred to a cryostat cooled to 93 K quickly enough not to raise the temperature of the sample.

For these samples, temperature dependences of the triplet decay rate were measured at temperatures between 93 K and 423 K while continuously raising the temperature at a rate of 3 K/min.

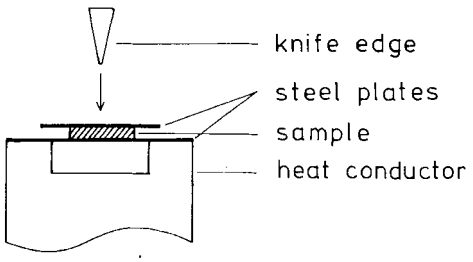

FIGURE 1 Method of mechanical deformation of samples. The sample is bent by the knife edge: then the edge is removed.

2.2. Measurement of anneal characteristics

For the mechanically-deformed samples, the deformation was made in the air at room temperature using the same method as previously. Isothermal annealing was performed at seven specified temperatures between 373 K and 403 K. For a quantitative analysis, measurements of the dislocation density must be made at a constant temperature for all the samples. Then, annealing was carried out by transferring the sample into a temperature-controlled furnace, and measurement of the triplet decay rate was made at 293 K after the sample was removed from the furnace for every sample.

This somewhat troublesome method results from the fact that the temperature of the trap stage is lower than the anneal temperature. This relationship between the temperatures is contrary to the results for X-ray irradiation damage.[12,13]

For the thermally-stressed samples, thermal defects were annealed at below room temperature, except for those corresponding to the dislocations observed in the mechanically-deformed samples. Compared to the experiment for the mechanically-deformed samples, it is difficult to perform the same anneal experiment at temperatures below room temperature. Therefore, measurements were taken only at those temperature ranges at which the defects were annealed.

3. EXPERIMENTAL RESULTS

Many cracks, which did not disappear even after annealing, were generated by thermal stress. On the other hand, no changes could be observed visually in the mechanically-deformed samples. The percentage recovery for the triplet exciton traps is about 80% overall for the mechanically-deformed samples as shown in Figure 2. This is almost the same value as that for the thermally-stressed samples. This means that macroscopic defects had virtually no influence on the triplet exciton on the whole. The variation in percentage recovery is similar for both (001)[100] and (001)[010] dislocations. Complete recovery is prevented by diffusion of air molecules promoted along dislocations and subgrain boundaries,[14] photodimerization at defects,[15] or polygonization. These effects become small rapidly with time or as the dislocation recovers, so that they do not seem to have a serious influence on the following analysis of trapping and annealing.

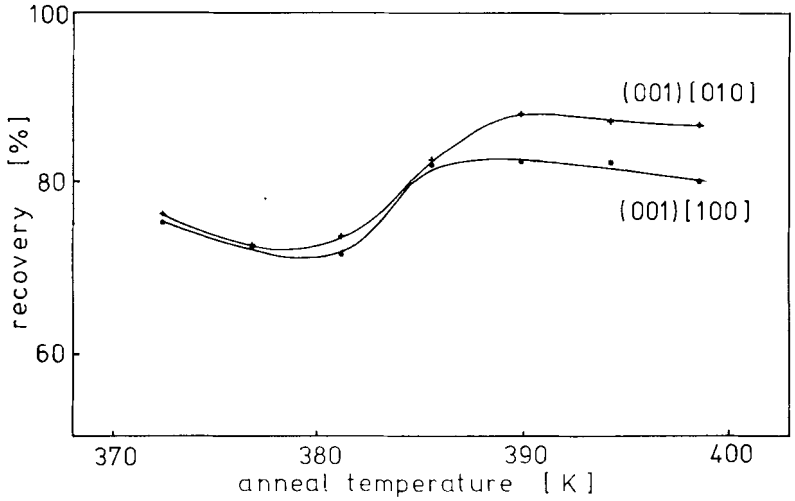

FIGURE 2 Percentage recovery of dislocations induced by plastic bending for each annealing temperature.

3.1. Analysis of trap stages

The temperature dependence of the triplet decay rate was measured successively between 93 K and 203, 223, 253, 333, and 423 K, labeled B203, B223, etc. in Figure 3. They are averages for the five samples. In order to exclude the influence of any other lattice defect or impurity, the trap stages are shown as the differences in the triplet decay rates before and after annealing of the defects corresponding to the individual trap stages. The stages in Figure 3 are trap stages but not anneal stages, since repeated measurements made on the same sample below the individual anneal temperature gave the same characteristics. It was found from Figure 3 that thermal defects were annealed or changed in physical nature at 93–203 K (corresponding to a stage I trap), 223–253 K (stage II), and 333–423 K (stages III, IV, and V).

In order to obtain the properties of the triplet exciton traps, the temperature dependence of the triplet decay rate $\beta(T)$ was analyzed using the following equations,[7]

$$\beta(T) = \beta_0 + \sum_i p_i\beta_i/(\beta_i + q_i), \tag{1}$$

$$q_i = q_0 \exp(-E_{Ti}/k_B T), \tag{2}$$

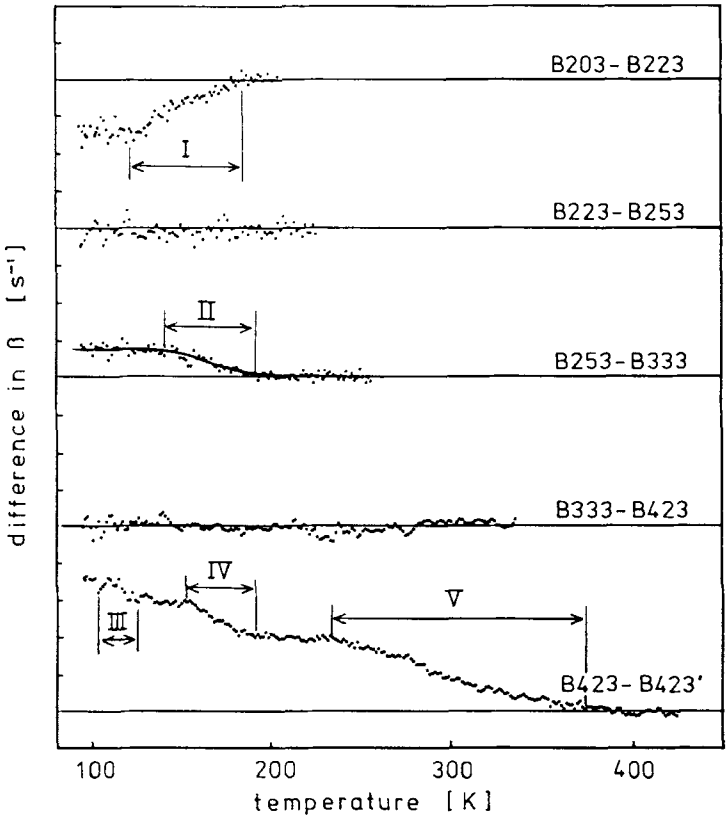

FIGURE 3 Triplet exciton trap stages in the thermally-stressed sample. B203 indicates the temperature dependence of the triplet decay rate with the temperature raised from 93 K to 203 K at a rate of 3 K/min. B423′ indicates a second measurement of B423. The measurements were made in order from lowest to higher final temperatures. The ordinate shows the difference in the triplet decay rate of them in 10 s^{-1}/1 div. The horizontal lines show the zero level for each stage. Trap stages are shown by Roman numerals in the figure. The solid line shows the result of curve fitting.

where subscript i is the stage number, β_0 is the triplet decay rate in the absence of traps, β_i is the triplet decay rate at the trap, q_i is the escape rate of the trapped triplet exciton, q_0 is the frequency factor (1×10^{12} s^{-1} is used here),[7] p_i is the trapping rate which is proportional to the trap density, E_{Ti} is the trap depth, k_B is Boltzmann's constant, and T is the temperature. Equation (1) is valid when the density of the trapped triplet excitons is much smaller than the total triplet density.

In stage I, the polarity of the change before and after annealing is different from any other stage. The following two completely opposite

causes are possible: A longlife trap was annealed; a shortlife trap was created in an already thermally-deformed region. If the change depends on the former cause, the triplet decay rate of the trap must be small compared to $\beta(T)$, $\sim 200\ s^{-1}$, measured after annealing, and the trap cannot be analyzed by Eq. (1). But if the latter cause holds, applying the equations to the polarity-changed data, a trap depth of 0.18 eV, and a triplet decay rate of $1 \times 10^6\ s^{-1}$, is obtained by curve fitting. For stage II, these parameters are 0.21 eV and $3.7 \times 10^5\ s^{-1}$; the result of the curve fitting is shown in Figure 3 by the solid line. The traps annealed below room temperature have no counterpart in the traps which have been reported up to now.

Stages III, IV, and V are almost the same as those observed in the mechanically-deformed samples discussed below. The traps observed in the thermally-stressed samples contain probably all the traps observed in the mechanically-deformed samples.

The dislocations introduced by plastic bending were annealed at above 363 K. The trap stages, i.e. the temperature dependencies of the difference in the triplet decay rates before and after annealing are displayed in Figure 4. The characteristics of the two dislocations are normalized to stage V. No longlife trap was observed in the temperature range measured. For stage III, the data is not precise enough for analysis. The results of curve fitting using Eqs. (1) and

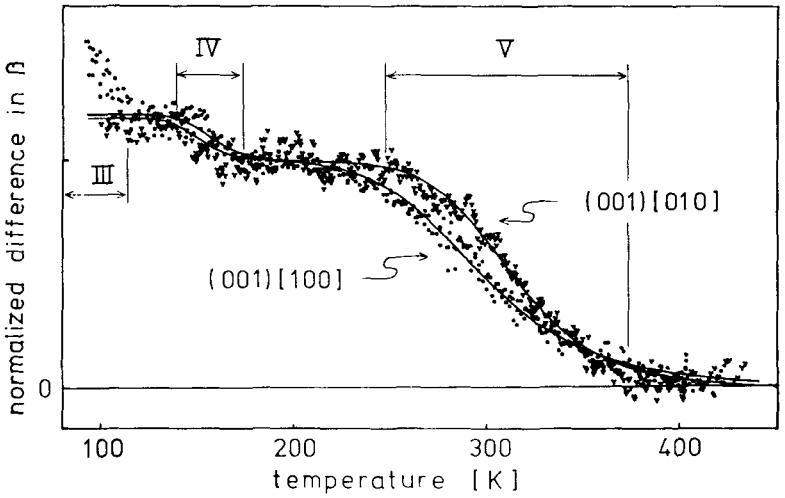

FIGURE 4 Triplet exciton trap stages in the mechanically-deformed samples. The ordinate is the difference in the triplet decay rate before and after annealing, normalized to the magnitude of stage V. The solid lines show the results of curve fitting.

(2) are shown by the solid lines in Figure 4; and the parameters used are listed in Table I.

Though stages III and IV have not been reported even in very similar experiments,[3,8,9] stage V agrees with those findings, but the analysis yields different results. This discrepancy may arise from inaccuracies due to the small S/N ratio at low temperatures and the differences in the recovery percentage and in the method of analysis, i.e. the difference in the triplet decay rate before and after annealing was used here. Since (001)[010] and (001)[100] are basal edge dislocations, they occur in all crystals grown by various methods. Triplet exciton traps with depths of 0.25–0.58 eV have been reported in many papers.

3.2. Analysis of the anneal characteristics

The anneal characteristics of dislocations introduced by plastic bending were analyzed from the relationship between anneal time and triplet decay rate using the following relations,

$$\beta(T,t) = \beta(T,\infty) + p_i(T,0)\exp(-k_i t), \tag{3}$$

$$k_i = k_{0i}\exp(-E_{Ri}/k_B T), \tag{4}$$

where k_i is the rate of recovery, k_{0i} is the frequency factor, t is the anneal time, and E_{Ri} is the activation energy of recovery. The method of analysis is essentially the same as that reported previously,[12,13] but the final value $\beta(T,\infty)$ was calculated by regression analysis instead of measurement after sufficient annealing.

The triplet decay rate was measured at 293 K after every anneal, and only defects corresponding to trap stage V are observable. The results of isothermal annealing are shown in Figure 5(a) and (b). They show that the anneal characteristics of the dislocations are first order

TABLE I

Trap depths and decay rates of the triplet exciton at the edge dislocations, which are derived from the data in Fig. 4 and eqs. (1) and (2) by curve fittings.

dislocations	(001) [100]	(001) [010]
E_{T4} [eV]	0.24	0.24
β_4 [s^{-1}]	2×10^4	1×10^4
E_{T5} [eV]	0.26	0.37
β_5 [s^{-1}]	3.9×10^7	1.1×10^6

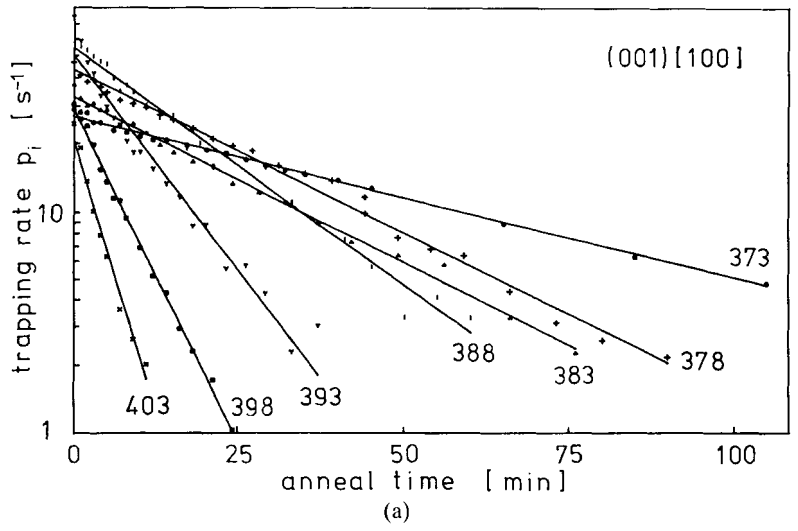

(a)

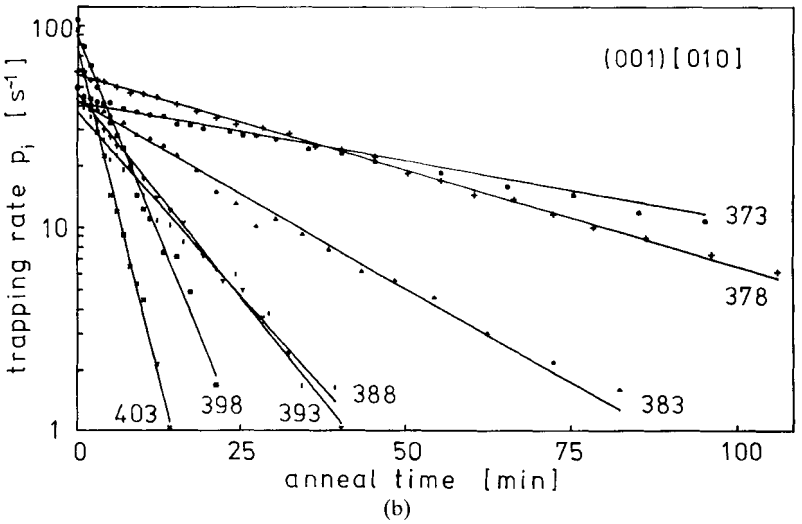

(b)

FIGURE 5(a), 5(b) Isothermal anneal characteristics of the dislocations. Figures (a) and (b) are for (001) [100] and (001) [010] edge dislocations, respectively. Anneal temperatures in degrees Kelvin are shown in the figures.

processes. The slope for each anneal temperature corresponds to the recovery rate expressed by eq. (4). A plot of the recovery rates in Figure 6 leads to the results shown in Table II. The Debye temperature of the anthracene crystal is about 100 K, and the frequency

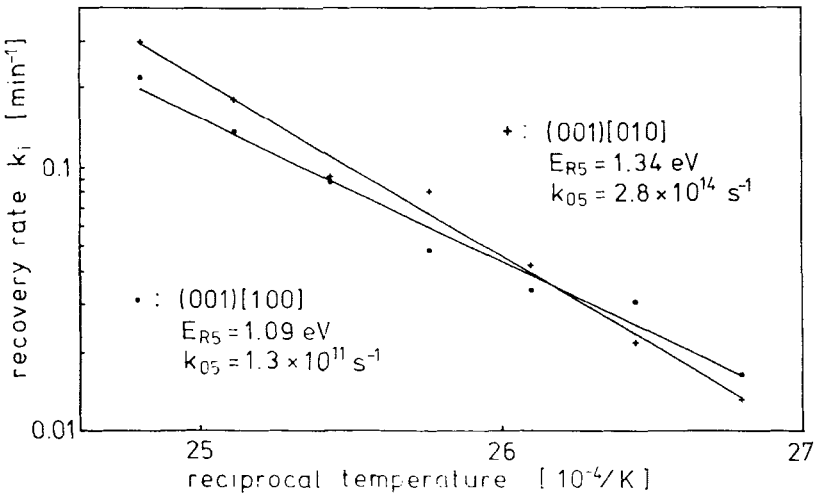

FIGURE 6 Recovery rates for the dislocations at various anneal temperatures. Results of analysis using eq. (4) are shown in the figure.

factor k_{0i} is assumed constant over the full temperature range measured.

4. DISCUSSION

It is not known at present whether the annealed (or created) exciton trap in stage I is radiative or nonradiative, so the cause cannot be decided by either the decay rate or the intensity of the delayed fluorescence. To clarify this, the defect phosphorescence must be observed. But stage I depends on a less disturbed defect than stage II, since the temperature ranges of the trap stage and annealing are lower, and the triplet decay rate is much smaller than those of the stage II. The defect corresponding to stage II is not an edge dislo-

TABLE II

Activation energies and frequency factors of recovery of the edge dislocations, which are derived from the data in Fig. 6 and eq. (4).

dislocations	(001) [100]	(001) [010]
E_{R5} [eV]	1.09	1.34
k_{05} [s^{-1}]	1.3 × 10^{11}	2.8 × 10^{14}

cation, since it was annealed at lower temperature than those for stages III, IV, and V, which are the edge dislocations with the lowest formation energy.[18] Even if it is a point defect, it may not be a vacancy, since the dilute region around the vacancy cannot trap excitons and self-diffusion is negligible below the anneal temperature.[14,19] They are displaced and/or misoriented regions of a few or more molecules, or screw dislocations: the self energy of (001)[010] screw dislocations is smaller than for any other edge dislocations.[18]

Stage V in the thermally-stressed sample is situated between stage V for the two edge dislocations; and the same trend was observed in a sample bent along both the *a* and *b* axes. The apparent trap depth is about 0.3 eV in both cases, and so they are thought to be mixtures of the two edge dislocations. However it cannot be confirmed whether stages III, IV, and V of the thermally-stressed sample contain no other defects, such as partial edge dislocation (001)1/2[110], which has an intermediate self-energy between edge dislocations (001)[100] and (001)[010].

The theory of trap formation for excitons differs from that for charge carriers: The former relates to dispersion and resonance energies and the latter to polarization energy. However, the hydrostatic pressure dependence of the calculated energy level shift[20,21] shows the same trend in both cases. The pressure dependence of the triplet level[22] is much smaller than that for the singlet level.[23] Applying the phenomenon of pressure effect to a compressed region of the dislocation, and using the results calculated by Sworakowski[20] on the polarization energy of an idealized (001)[010] edge dislocation, the trap depth of the triplet exciton is estimated to be smaller than 0.05 eV. An independent theoretical estimation by Crisp and Walmsley[24] of exciton trap depths associated with orientationally disordered regions supports this result. In addition to this, the relation between the trap depths measured for edge dislocations (001)[100] and (001)[010] is contrary to the result estimated by the amounts of molecular displacement, i.e. lattice constants 8.58 and 6.02 A, respectively. This indicates that trap stages II–V relate to excited states of extended defect regions, e.g. triplet excimer at a so-called incipient dimer proposed by Goode et al.[8] and supported by Arnold and Hassan.[17]

Singlet excimer emission has been observed under static high pressure by Tanaka et al.[25] and in crystals with disordered regions induced by photodimerization by Williams et al.[26] Since trap depths for the singlet exciton are about 4000 cm^{-1} (0.5 eV), from the relation between trap depths for the singlet and the triplet exciton mentioned

above, the singlet excimer possibly corresponds to the defect for stage V in this experiment.

Because the vibrational relaxation is much faster than the escape rate of the trapped exciton, neither stages III or IV correspond to any higher vibronic state of stage V. Stages III–V disappear at the same time with annealing; The ratio of the magnitude of stage IV and stage V almost agrees in all samples. These facts mean that the edge dislocations and any other possible defects consist of three or more fundamental exciton traps. These traps may correspond to extended defect regions with a different degree of misorientation or displacement around their cores. Three singlet excimers were observed by Hofmann et al.[27] in sublimation layers, but the relationship between these singlet excimers and our stages III–V is not clear.

Though the exciton trap depth relates to the interaction energy of a molecule or molecules in the excited state at the defect site with the surrounding molecules, the recovery energy relates to the interaction energy in the ground state. In stage V, which corresponds to the deepest trap, i.e. possibly the nearest trap to the dislocation core, the ratio of the trap depth to the recovery energy roughly agrees in both dislocations. While this relationship itself does not lead to any result about the dislocations, an enhanced anneal effect due to photoillumination, if it exists, will give further information about excited states and a change of molecular configurations at the defect sites.

Self-diffusion energy measured by the radioactive tracer method[14,19] is about 0.9 eV*; formation energies calculated for the (001) [100] and (001) [010] edge dislocations are 2.2 and 4.0 eV for one molecular plane, respectively.[28] The recovery energies of the dislocations are smaller than the formation energies, but reasonably larger than the self-diffusion energy, since the dislocation cores are larger than one molecule.

Since the frequency factor of the recovery for the (001) [010] edge dislocation exceeds the lattice phonon frequency $\sim 10^{12}\ s^{-1}$, we consider that the defect recovery is due mainly to vibrational coupling among the various vibrational modes including intermolecular and intramolecular vibrations (up to $\sim 10^{14}\ s^{-1}$).

As long as structural imperfections are accompanied by an orientational change of anisotropic molecules, as occurs in most organic molecular crystals, the activation energy on recovery may not be

*Self diffusion in bulk anthracene has $E_A \sim 2$ eV (Ref. J. N. Sherwood & D. J. White, *Phil. Mag.* **15** 745 1967)

expressed as simply as that for formation and movement of a kink or Peierls potential in inorganic crystals.

Acknowledgement

We would like to thank Dr. M. Terada for making the anthracene crystals and Mr. H. Kawajiri for his help with the experiments.

References

1. W. Siebrand, *J. Chem. Phys.*, **42**, 3951 (1965).
2. S. Singh and F. R. Lipsett, *J. Chem. Phys.*, **41**, 1163 (1964).
3. S. Arnold, W. B. Whitten and A. C. Damask, *J. Chem. Phys.*, **53**, 2878 (1970).
4. G. C. Smith, *Phys. Rev.*, **166**, 839 (1968).
5. D. H. Goode and F. R. Lipsett, *J. Chem. Phys.*, **51**, 1222 (1969).
6. Z. Zboinski, *Phys. Status Solidi b*, **87**, 663 (1978).
7. K. Yokoi and Y. Ohba, *Jpn. J. Appl. Phys.*, **19**, 1655 (1980).
8. D. Goode, Y. Lupien, W. Siebrand, D. F. Williams, J. M. Thomas and J. O. Williams, *Chem. Phys. Lett.*, **25**, 308 (1974).
9. A. Sasaki and S. Hayakawa, *Jpn. J. Appl. Phys.*, **17**, 283 (1978).
10. K. Kojima, K. Okamoto and S. Takeuchi, *J. Cryst. Growth*, **67**, 149 (1984).
11. P. M. Robinson and H. G. Scott, *Phys. Status Solidi*, **20**, 461 (1967).
12. K. Yokoi and Y. Ohba, *Chem. Phys. Lett.*, **56**, 560 (1978).
13. K. Yokoi and Y. Ohba, Oyo Buturi, **47**, 649 (1978) [in Japanese.]
14. P. J. Reucroft, H. K. Kevorkian and M. M. Labes, *J. Chem. Phys.*, **44**, 4416 (1966).
15. P. E. Schipper and S. H. Walmsley, *Proc. R. Soc.*, London A, **348**, 203 (1976).
16. J. O. Williams and Z. Zboinski, *J. Chem. Soc.*, Faraday II, **74**, 618 (1978).
17. S. Arnold and N. Hassan, *J. Chem. Phys.*, **78**, 5606 (1983).
18. K. Kojima, *Phys. Status Solidi* a, **51**, 71 (1979).
19. C. H. Lee, H. K. Kevorkian, P. J. Reucroft and M. M. Labes, *J. Chem. Phys.*, **42**, 1406 (1965).
20. J. Sworakowski, *Mol. Cryst. & Liq. Cryst.*, **33**, 83 (1976).
21. P. E. Schipper, *Mol. Cryst. & Liq. Cryst.*, **28**, 401 (1974).
22. S. Arnold, W. B. Whitten and A. C. Damask, *J. Chem. Phys.*, **61**, 5162 (1974).
23. R. Sonnenschein, K. Syassen and A. Otto, *J. Chem. Phys.*, **74**, 4315 (1981).
24. G. M. Crisp and S. H. Walmsley, *Mol. Cryst. & Liq. Cryst.*, **58**, 71 (1980).
25. J. Tanaka, T. Koda, S. Shionoya and S. Minomura, *Bull. Chem. Soc. Jpn.*, **38**, 1559 (1965).
26. J. O. Williams, D. Donati and J. M. Thomas, *J. Chem. Soc.* Faraday II, **73**, 1169 (1977).
27. J. Hofmann, K. P. Seefeld, W. Hofberger and H. Bassler, *Mol. Phys.*, **37**, 973 (1979).
28. E. A. Silinsh, *Organic Molecular Crystals* (Springer, Berlin, 1980) p. 166.